ChemPubSoc Europe

DOI: 10.1002/ejoc.201900107

EurJOC European Journal of Organic Chemistry

Full Paper

Asymmetric Hydroamination

Rare-Earth-Metal-Catalyzed Kinetic Resolution of Chiral Aminoalkenes via Hydroamination: The Effect of the Silyl Substituent of the Binaphtholate Ligand on Resolution Efficiency

Hiep N. Nguyen[a] and Kai C. Hultzsch*[b]

Abstract: The kinetic resolution of α-substituted aminopentenes via intramolecular hydroamination was investigated using various 3,3′-silyl-substituted binaphtholate yttrium catalysts. High efficiencies in the kinetic resolution were observed for methyl-, benzyl-, and phenyl-substituted substrates utilizing the cyclohexyldiphenylsilyl-substituted catalyst **2c** with resolution factors reaching as high as 90(5) for hex-5-en-2-amine (**3a**). Kinetic analysis of the enantioenriched substrates with the matching and mismatching catalyst revealed that the efficiency of catalyst **2c** benefits significantly from a favorable Curtin–Hammett pre-equilibrium and by a large k_{fast}/k_{slow} ratio. Other binaphtholate catalysts were less efficient due to a less favorable Curtin–Hammett pre-equilibrium, which often favored the mismatching substrate-catalyst combination. Cyclization of the matched substrate proceeds generally with large *trans*-selectivity, whereas the *trans*/*cis*-ratio for mismatched substrates is significantly diminished, favoring the *cis*-cyclization product isomer in some instances.

Introduction

Nitrogen-containing compounds are widely found in nature and biological systems; therefore, this class of organic compounds is of high importance in fundamental research, as well as pharmaceutical and chemical industry.[1] The metal-catalyzed hydroamination of olefins, in which an amine N–H functionality adds directly to an unsaturated carbon–carbon bond, provides one of the simplest routes to amine products with 100 % atom efficiency.[2] Significant research efforts have resulted in the development of a large variety of catalyst systems for the hydroamination of olefins;[3–8] however, many challenges remain, in particular with respect to asymmetric hydroamination reactions.[9–11]

We have developed biphenolate, binaphtholate and NOBIN-based aminophenolate rare-earth metal catalysts for the asymmetric intra-[12] and intermolecular[12e,12f,13] hydroamination of alkenes. In particular 3,3′-bis(silyl)-substituted binaphtholate rare-earth metal complexes (Figure 1) exhibited high activity and enantioselectivities of up to 96 % *ee* in intramolecular reactions and up to 66 % *ee* in intermolecular reactions.[12d,12f,13]

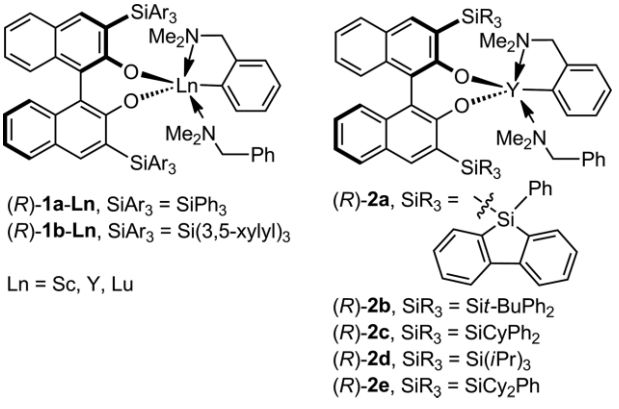

Figure 1. Rare-earth metal complexes based on 3,3′-bis(silyl)-binaphtholate ligands for asymmetric hydroamination reactions.

Moreover, complexes **1a** and **1b** were also applied in the catalytic kinetic resolution of chiral aminoalkenes via the asymmetric hydroamination/cyclization (Scheme 1).[12c,12d,14–17]

Previously we have shown that resolution factors *f* as high as 19 can be achieved for a phenyl-substituted aminopentene using (*R*)-**1a-Lu** at 40 °C (Scheme 1, R = Ph).[12d,15] The hydroamination products of aryl-substituted aminopentenes using the binaphtholate catalysts **1a** and **1b** displayed high *trans*/*cis* diastereoselectivity of up to 50:1. Moreover, the kinetic study of the kinetic resolution process revealed that the Curtin–Hammett pre-equilibrium favors the matching substrate-cata-

[a] *Rutgers, The State University of New Jersey, Department of Chemistry and Chemical Biology*
610 Taylor Road, Piscataway, New Jersey 08854-8087, USA
[b] *Universität Wien, Fakultät für Chemie, Institut für Chemische Katalyse*
Währinger Straße 38, 1090 Wien, Austria
E-mail: kai.hultzsch@univie.ac.at
https://chemcat.univie.ac.at/

Supporting information and ORCID(s) from the author(s) for this article are available on the WWW under https://doi.org/10.1002/ejoc.201900107.

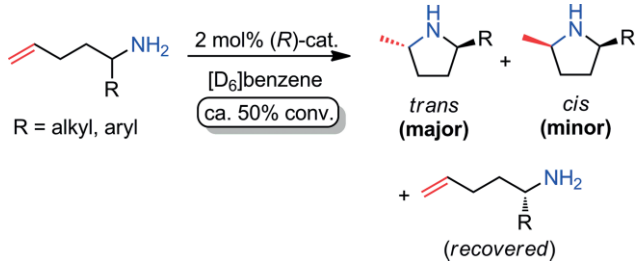

Scheme 1. General scheme of the kinetic resolution of α-substituted aminoalkenes.

lyst complex for α-substituted aminopentenes containing aryl substituents, as indicated by a pre-equilibrium constant K^{dias} > 1 (vide infra). However, the kinetic resolution of aminoalkene substrates containing aliphatic substituents in the α-position of the amine was significantly less efficient with these catalysts, primarily as a result of a shifted Curtin–Hammett pre-equilibrium in favor of the mismatching substrate-catalyst complex (K^{dias} < 1).

Herein we report the kinetic resolution process using the yttrium catalysts (*R*)-**2a**–**e**[12f] based on binaphtholate ligands with a variety of bulky trisarylsilyl-, trialkylsilyl-, and alkylarylsilyl-substituents in the 3 and 3′ position (Figure 1). Our previous studies have shown that the sterically demanding silyl groups in the binaphtholate catalysts are responsible for catalyst stability as well as high catalytic activity and selectivity, but herein we will show that subtle changes in these silyl-substituents can have a significant influence on the kinetic resolution process, especially on the Curtin–Hammett pre-equilibrium.

Results and Discussion

Previously we had observed that the cyclization of α-substituted aminopentenes proceeds significantly faster using the triphenylsilyl-substituted binaphtholate catalyst (*R*)-**1a-Y** compared to (*R*)-**1a-Lu** and that (*R*)-**1a-Y** displayed slightly higher efficiency in the kinetic resolution of the sterically less demanding substrate **3a** in comparison to the smaller ionic radius metal complex (*R*)-**1a-Lu** (Table 1, entries 1, 2).[12c,12d,15] We therefore decided to focus our kinetic resolution studies on the more active and presumably more efficient yttrium catalysts (*R*)-**2a**–**e**. A broad range of substrates for intra- and intermolecular asymmetric hydroamination reactions unrelated to the kinetic resolution process has been reported for these catalysts recently.[12f] For the purpose of this study we investigated the kinetic resolution of the racemic α-substituted 1-aminopent-4-enes **3a**–**d** (Table 1). These substrates feature aliphatic as well as aromatic substituents which had been kinetically resolved with low (resolution factor *f* = 2–6 for **3b**, **3d**) to moderate (*f* = 6–19 for **3a**, **3c**) efficiency using catalysts (*R*)-**1a-Ln** and (*R*)-**1b-Ln**.[12c,12d,15]

For the sterically least demanding methyl-substituted aminopentene **3a**, the structurally rigid dibenzosilole-substituted complex (*R*)-**2a** was more efficient than the triphenylsilyl-substituted binaphtholate catalysts (*R*)-**1a-Y** and (*R*)-**1a-Lu** (Table 1, entries 1–3). The sterically more demanding dicyclohexylphenylsilyl-substituted binaphtholate complex (*R*)-**2e** showed significantly diminished kinetic resolution efficiency (Table 1, entry 5), while exhibiting a significant higher rate of cyclization in comparison to the other catalysts. Remarkably, the cyclohexyldiphenylsilyl-substituted binaphtholate complex (*R*)-**2c** was significantly more efficient than all other binaphtholate complexes **1** and **2** with a resolution factor *f* > 50[18] for **3a** (Table 1, entry 4). Although the silyl groups in the 3 and 3′ positions of the binaphtholate ligands had a pronounced effect on catalytic activity as well as the resolution factors in the cyclization of **3a**, the *trans*/*cis* diastereoselectivities were rather unaffected, showing consistently low ratios in the range of 7:1 to 9:1.

Higher *trans*/*cis* selectivities of up to 20:1 were observed for the benzyl-substituted aminopentene **3b** (Table 1, entries 6–9). However, the cyclization of **3b** proceeded at a much lower rate using the *tert*-butyldiphenylsilyl-substituted binaphtholate catalyst (*R*)-**2b** in comparison to (*R*)-**1a-Y** [42.3 h at 25 °C for (*R*)-**2b** vs. 9 h at 22 °C for (*R*)-**1a-Y** to obtain 50 % conversion; see Table 1, entries 6 and 8]. This is in contrast to our observation that (*R*)-**2b** generally displayed similar catalytic activity as (*R*)-**1a-Y** in the cyclization of aminopentenes.[12f] Despite the slow rate of cyclization, (*R*)-**2b** resolved **3b** more efficiently than (*R*)-**1a-Y**. Similar to the previous observation, the resolution of **3b** was generally less efficient than the resolution of **3a** with the same rare-earth metal binaphtholate catalyst (for example, compare Table 1, entry 4 and 9). Nevertheless, catalyst (*R*)-**2c** resolved **3b** with a still impressive resolution factor of 43.

The kinetic resolution of the phenyl-substituted aminopentene **3c** was performed at 40 °C using catalysts (*R*)-**2a**–**e** with good turnover rates, giving consistently high *trans*/*cis* selectivities ≥ 50:1 (Table 1, entries 11–15). Complexes (*R*)-**2a**, (*R*)-**2b**, and (*R*)-**2c** displayed similar catalytic activity in the cyclization of **3c** (Table 1, entries 11–13), but as for substrates **3a** and **3b**, the highest resolution factor (*f* > 50) was observed for the cyclohexyldiphenylsilyl-substituted binaphtholate complex (*R*)-**2c**. As expected, the triisopropylsilyl-substituted binaphtholate catalyst (*R*)-**2d** exhibited the lowest activity as well as the lowest efficiency in the resolution of **3c** (Table 1, entry 14) in agreement to its general performance in the hydroamination/cyclization of achiral aminopentenes.[12f] The dicyclohexylphenylsilyl-substituted complex (*R*)-**2e** exhibited the highest activity in the cyclization of **3c** at three times the rate compared to (*R*)-**2a**–**c** (Table 1, entries 11–13 vs. entry 15), but unfortunately at the expense of resolution efficiency.

Previous studies have shown that the sterically more demanding α-alkyl substrates, such as the benzyl-substituted **3b** and the cyclohexyl-substituted **3d** exhibit significantly diminished resolution factors using the bis(triarylsilyl)-substituted binaphtholate catalysts (*R*)-**1a-Ln** and (*R*)-**1b-Ln**.[15] This observation is also true for **3d** using the cyclohexyldiphenylsilyl-substituted binaphtholate catalyst (*R*)-**2c** (Table 1, entry 19). Interestingly, the least reactive, triisopropylsilyl-substituted catalyst (*R*)-**2d** resolved **3d** most effectively among our available binaphtholate catalysts, with a resolution factor of 8.9 (Table 1, entry 20). Among all the tested substrates, cyclization of **3d** proceeded with the lowest *trans*/*cis* diastereoselectivity in the range of 5:1–10:1.

Table 1. Catalytic kinetic resolution of α-substituted 1-aminopent-4-enes.[a]

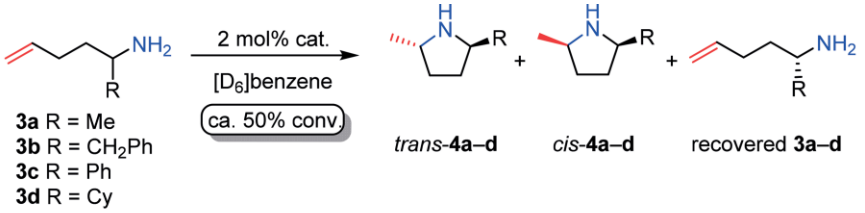

Entry	Subst.	Cat.	T [°C]	t [h]	Conv. [%]	trans/cis[b]	ee [%][c]	f
1	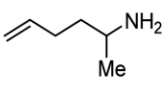 3a	(R)-1a-Y	22	25.5	53	11:1	72	9.5[d]
2		(R)-1a-Lu	22	42	55	10:1	73	8.4[d]
3		(R)-2a	25	29.5	49	9:1	71	14
4		(R)-2c	25	13.0	48	7:1	86	>50
5		(R)-2e	25	4	50	8:1	34.5	2.8
6	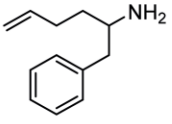 3b	(R)-1a-Y	22	9	50	20:1	42	3.6[d]
7		(R)-1b-Y	22	27	52	20:1	38	2.9[d]
8		(R)-2b	25	42.3	50	20:1	64	8.6
9		(R)-2c	25	17.8	48	20:1	82	43
10	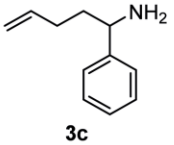 3c	(R)-1a-Y	22	95	50	≥50:1	74	15[d]
11		(R)-2a	40	41.0	50	≥50:1	77	18
12		(R)-2b	40	39	54	≥50:1	86	18
13		(R)-2c	40	39	46	≥50:1	78	>50
14		(R)-2d	40	82	50	≥50:1	30	2.4
15		(R)-2e	40	14	45	≥50:1	57.5	10
16	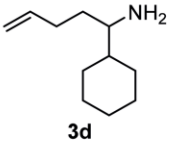 3d	(R)-1a-Y	22	8	56	---	49	3.5[e]
17		(R)-1b-Y	22	46	59	---	54	3.6[e]
18		(R)-2b	25	3.3	54	5:1	56	4.8
19		(R)-2c	25	4.3	51	7:1	57	5.9
20		(R)-2d	25	16	58	10:1	80	8.9
21		(R)-2e	25	5.5	50	6:1	41	3.5

[a] General reaction conditions: 0.10–0.20 mmol substrate ([sub.] = 0.2–0.5 M), 2 mol-% cat., [D6]benzene, Ar atm. [b] *Trans*/*cis* ratio of products. [c] Enantiomeric excess of recovered starting material **3a**–**d**. [d] Data from ref.[12d] [e] Data from ref.[15]

In order to identify the factors governing the high efficiency of the cyclohexyldiphenylsilyl-substituted binaphtholate complex (*R*)-**2c** in the kinetic resolution process, we started a more detailed investigation of the kinetic resolution of aminoalkenes using the general model (Scheme 2).[12d,15,19]

The two diastereomeric substrate-catalyst complexes [*cat*-*S*] and [*cat*-*R*] readily interconvert with an equilibrium constant K^{dias} (Equation 1) and each of the complexes reacts with a corresponding rate constant (k_R and k_S) to give the corresponding hydroamination products. The rate of interconversion between

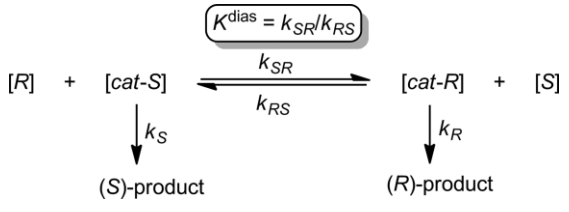

Scheme 2. The general model for the kinetic resolution of aminoalkenes ([*S*], [*R*] = substrate enantiomers; [cat-*S*], [cat-*R*] = substrate-catalyst complex of respective substrate enantiomer).

the two substrate-catalyst complexes is rapid even at low temperatures and significantly higher than both rates of cyclization.[12d]

$$K^{dias} = \frac{k_{SR}}{k_{RS}} = \frac{[cat-R][S]}{[cat-S][R]} \quad (1)$$

The resolution factor *f* is determined by the equilibrium constant K^{dias} and the cyclization rate constants of the two diastereomeric substrate-catalyst complexes (Equation 2),[20] which may be determined independently.

$$f = K^{dias}\frac{k_R}{k_S} \quad (2)$$

For pseudo-first-order reactions the resolution factor can be expressed as a function of conversion *C* and *ee* of recovered substrate (Equation 3).[19]

$$f = \frac{ln[(1-C)(1-ee)]}{ln[(1-C)(1+ee)]} \quad (3)$$

According to Equation 3, the resolution factor *f* for **3a** using the binaphtholate catalyst (*R*)-**2c** can be determined by plotting ln[(1–*C*)(1 – *ee*)] vs. ln[(1–*C*)(1 + *ee*)] (Figure 2). The relationship between conversion and enantiomeric excess *ee* is expressed by Figure 3.

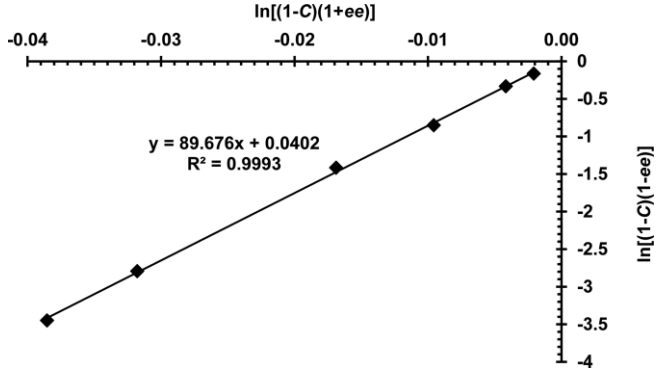

Figure 2. Plot of ln[(1–*C*)(1 – *ee*)] vs. ln[(1–*C*)(1 + *ee*)] for the kinetic resolution of **3a** using binaphtholate catalyst (*R*)-**2c** at 25 °C.

Inspired by the high resolution factor for the methyl-substituted aminopentene **3a** obtained with the cyclohexyldiphenylsilyl-substituted binaphtholate catalyst (*R*)-**2c** at 25 °C, a large-scale kinetic resolution of **3a** was performed with (*S*)-**2c**, giving (*S*)-**3a** (95 % *ee*) in 38 % re-isolated yield at 52 % conversion. The yield of (*S*)-**3a** is lower than expected due to its volatility (b.p. 114–116 °C at 760 Torr). The enantioenriched α-substituted aminopentenes **3b**–**3d** were also prepared using (*R*)-**2c** and the resolution data are summarized in Table 2.

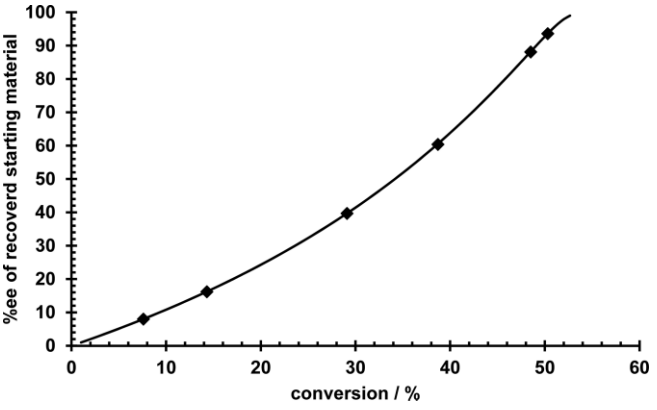

Figure 3. Dependence of enantiomeric excess of recovered starting material on conversion in the kinetic resolution of **3a** with (*R*)-**2c** at 25 °C. The line was fitted to a resolution factor *f* = 90.

The rate constants k_{fast} and k_{slow} for the cyclization of the matching and mismatching substrate-catalyst combination, respectively, were obtained via kinetic measurements of the cyclization rates of enantioenriched (*S*)-**3a** using (*R*)-**2c** (Figure 4) in the temperature range of 25–50 °C for the faster matching substrate-catalyst combination, respectively the cyclization of (*S*)-**3a** using (*S*)-**2c** (Figure 5) in the temperature range of 25–55 °C for the slower mismatching substrate-catalyst combination.

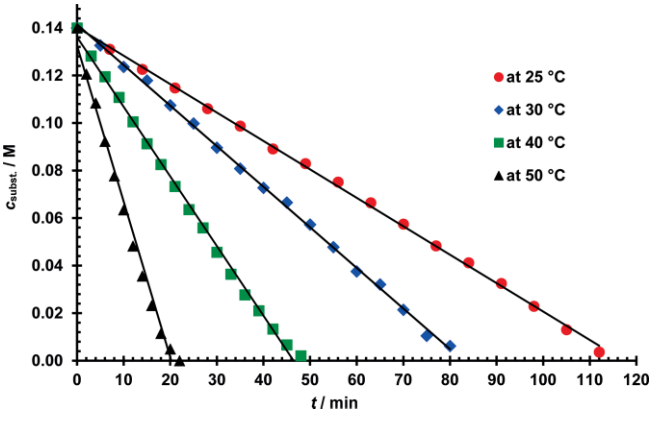

Figure 4. Time dependence of the substrate concentration in the hydroamination of (*S*)-**3a** using (*R*)-**2c** {matching pair; [(*S*)-**3a**]$_0$ = 0.140 mol L^{-1}, [(*R*)-**2c**] = 2.73 mmol L^{-1}}. The straight lines represent the least square linear regression.

The kinetic data and resolution parameters of α-substituted aminopentenes were determined with the alkylarylsilyl-substituted binaphtholate catalysts **2b**, **2c**, and **2e** (Table 3). In agree-

Table 2. Large-scale preparation of enantioenriched α-substituted aminopentenes via kinetic resolution using binaphtholate catalyst **2c**.[a]

Subst.	Cat.	*T* [°C]	*t* [h]	*f* [b]	Conv. [%]	Yield (*ee*, config.) [%][c]
3a	(*S*)-**2c**	25	9	90(5)	52	38 (95, *S*)
3b	(*R*)-**2c**	25	22.5	43	57	40 (95, *S*)
3c	(*R*)-**2c**	40	31	> 50	54	40 (97, *S*)
3d	(*R*)-**2c**	25	9.5	5.6(3)	77	18 (95, *S*)

[a] General reaction conditions: 0.8–1.5 g of racemic aminoalkene ([sub.] = 0.9–1.3 M), 2 mol-% cat., benzene, Ar. [b] Taken from Table 3 (for **3a** and **3d**) and Table 1 (for **3b** and **3c**). [c] Isolated yield and *ee* value of recovered (*S*)-**3**. All recovered aminoalkenes have (*S*) configuration, because the CIP priorities differ between substrate **3a** on the one side and substrate **3b**–**d** on the other side. Thus, the (*S*)-catalyst enantiomer is the matching catalyst for substrate (*R*)-**3a**, while it is the (*R*)-catalyst enantiomer for substrates (*R*)-**3b**–**d**.

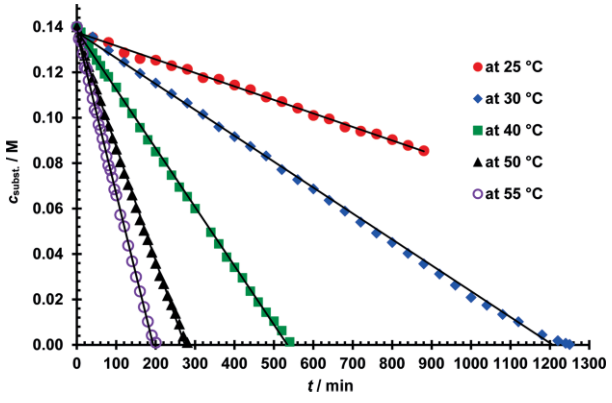

Figure 5. Time dependence of the substrate concentration in the hydroamination of (*S*)-**3a** using (*S*)-**2c** {mismatching pair; $[(S)\text{-}\mathbf{3a}]_0$ = 0.140 mol L^{-1}, $[(S)\text{-}\mathbf{2c}]$ = 2.73 mmol L^{-1}}. The straight lines represent the least square linear regression.

ment with the kinetic measurements reported previously for the methyl-substituted **3a** using the triphenylsilyl-substituted binaphtholate catalyst **1a-Y**,[15] the Curtin–Hammett pre-equilibrium favors the mismatching substrate-catalyst combination (K^{dias} < 1) when **3a** is paired with catalysts **2b** and **2e** (Table 3, entries 1, 2 and 7). On the contrary, the equilibrium for the cyclohexyldiphenylsilyl-substituted binaphtholate catalyst **2c** and substrate **3a** favors the matching substrate-catalyst complex (K^{dias} > 1); thus, effectively enhancing the efficiency of the kinetic resolution process. The relative rate k_{fast}/k_{slow} remains in the range of 9.1(3)–18.9(2) for the methyl-substituted aminopentene **3a** with our novel binaphtholate catalysts **2b**, **2c**, and **2e** at temperatures ranging from 25 to 50 °C, with the highest ratio being achieved with **2c** at 25 °C. Dramatic differences in the *trans*/*cis* diastereoselectivities in the cyclization of (*S*)-**3a** using (*R*)-**2c** (Figure 6, trace a, *trans*/*cis* = 39:1 for the matching

Table 3. Kinetic resolution parameters of α-substituted aminopentenes.[a]

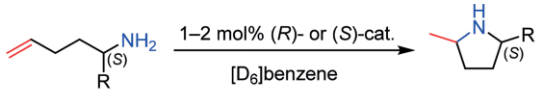

(*S*)-**3a** R = Me
(*S*)-**3b** R = CH_2Ph
(*S*)-**3c** R = Ph
(*S*)-**3d** R = Cy

trans and *cis*
4a–d

Entry	Subst.	Cat.	*T* [°C]	k_{fast} [10^{-3} s^{-1}][b]	k_{slow} [10^{-3} s^{-1}]	k_{fast}/k_{slow}	*f* [c]	K^{dias}	*trans*/*cis* fast (slow, conv.[d] [%])
1	**3a**	**1a-Y**	30	8.5	1.12	7.6	6.4	0.84	>30:1.0 (2.8:1.0, 100)[e]
2	**3a**	**2b**	25	2.31(1)	0.215(2)	10.7(1)	5.8(1)	0.54(1)	35:1.0 (2.2:1.0, 77)
3	**3a**	**2c**	25	7.35(5)	0.388(4)	18.9(2)	90(5)	4.8(3)	39:1.0 (1:1.2, 100)
4	**3a**	**2c**	30	10.26(5)	0.730(1)	14.1(1)	77(5)	5.5(4)	38:1.0 (1:1.25, 100)
5	**3a**	**2c**	40	19.3(1)	1.64(1)	11.8(1)	46(2)	3.9(2)	38:1.0 (1:1.3, 100)
6	**3a**	**2c**	50	47.2(6)	3.19(1)	14.8(2)	23.7(4)	1.60(3)	38:1.0 (1:1.2, 100)
7	**3a**	**2e**	25	3.08(1)	0.34(1)	9.1(3)	2.8(1)	0.31(1)	35:1.0 (1.5:1.0, 60)
8	**3b**	**1a-Y**	30	2.5	0.26	9.6	2.6	0.27	>30:1.0 (>30.0:1.0, 85)[e]
9	**3b**	**2b**	40	3.15(4)	0.432(4)	7.3(1)	6.1(4)	0.84(6)	24:1.0 (4.0:1.0, 65)
10	**3b**	**2c**	40	5.7(1)	0.437(8)	13.0(3)	32(1)	2.5(1)	25:1.0 (1.0:1.0, 70)
11	**3b**	**2e**	40	2.84(6)	0.542(7)	5.2(1)	5.5(1)	1.06(3)	21:1.0 (1.7:1.0, 77)
12	**3c**	**1a-Y**	60	11.3	1.59	7.1	11.5	1.6	>50:1.0 (8.8:1.0, 99)[f]
13	**3c**	**2b**	70	5.35(2)	0.48(1)	11.2(2)	11.6(6)	1.04(5)	>50:1.0 (3.2:1.0, 45)
14	**3c**	**2c**	60	3.76(2)	0.24(1)	15.7(7)	24.6(3)	1.57(7)	>50:1.0 (7.0:1.0, 30)
15	**3c**	**2c**	70	6.90(6)	0.46(1)	15.0(4)	16.6(8)	1.11(6)	>50:1.0 (6.9:1.0, 30)
16	**3c**	**2e**	70	3.91(3)	0.65(1)	6.0(1)	7.6(3)	1.27(5)	>50:1.0 (2.2:1.0, 100)
17	**3d**	**1a-Y**	30	8.5	1.0	8.5	2.7	0.32	9.0:1.0 (1.4:1.0, 90)[e]
18	**3d**	**2b**	25	4.47(5)	1.19(2)	3.76(8)	4.7(2)	1.25(6)	24:1.0 (1.0:2.4, 100)
19	**3d**	**2c**	25	3.12(1)	0.790(3)	3.95(2)	5.6(3)	1.42(8)	20:1.0 (1.0:1.9, 100)
20	**3d**	**2e**	25	1.93(1)	1.11(1)	1.74(2)	3.6(1)	2.07(4)	21:1.0 (1.2:1.0, 100)

[a] General reaction conditions: 58–74 μmol (*S*)-**3a**–**d** ([sub.] = 0.11–0.14 M), 2 mol-% cat., [D_6]benzene, Ar. [b] $k_{fast} = k_R$ for the reaction of (*S*)-**3a** with (*R*)-catalyst; $k_{fast} = k_S$ for the reaction of (*S*)-**3b**, (*S*)-**3c**, (*S*)-**3d** with (*S*)-catalyst. [c] Determined from the slope of plot of $\ln(1-C)(1-ee)$ vs. $\ln(1-C)(1+ee)$, with at least three data points. [d] Conversion for mismatching substrate at which *trans*/*cis* ratio was determined. [e] Data from ref.[15] [f] Data from ref.[12d]

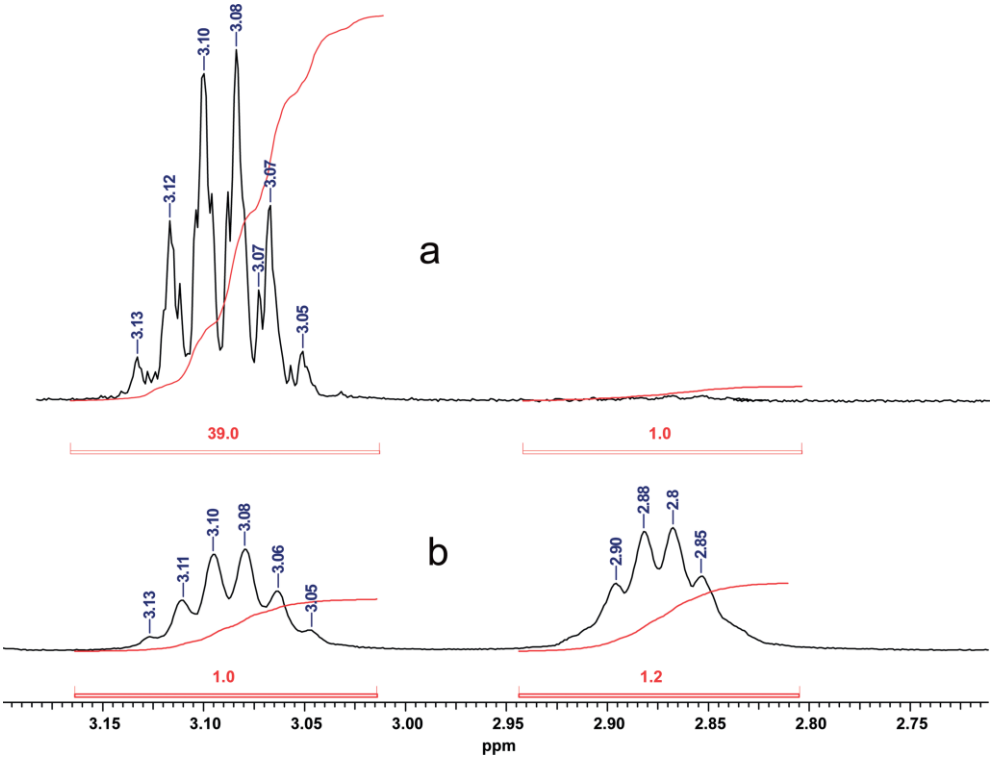

Figure 6. ^{1}H NMR spectra of hydroamination products **4a** obtained with the matching substrate–catalyst pair (*S*)-**3a** and (*R*)-**2c** (trace a) and with the mismatching substrate–catalyst pair (*S*)-**3a** and (*S*)-**2c** (trace b).

substrate–catalyst pair) and (*S*)-**3a** using (*S*)-**2c** (Figure 6, trace b, *trans*/*cis* = 1:1.2 for the mismatching substrate–catalyst pair) account for the low *trans*/*cis* selectivities observed in the kinetic resolution of racemic **3a** (*trans*/*cis* = 7–9:1, Table 1, entries 3–5). Additionally, the *trans*/*cis* ratios decrease gradually as the resolution reaction proceeds (Figure 7). It is noteworthy that the reaction of (*S*)-**3a** using (*S*)-**2c** (mismatching substrate–catalyst pair) preferentially produced the *cis*-product at all reaction temperatures in the range of 25–50 °C (Table 3, entries 3–6).

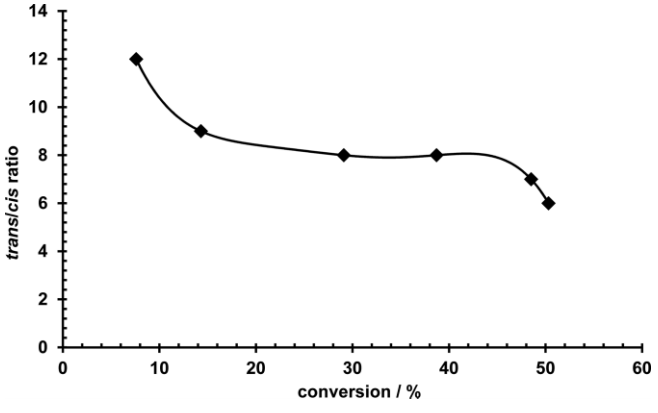

Figure 7. *trans*/*cis* ratio of **4a** formed in the kinetic resolution of *rac*-**3a** using 2 mol-% of (*R*)-**2c** at 25 °C as a function of conversion. The line is drawn as a guide for the eye.

In agreement to the observations for **3a**, the mismatching substrate-catalyst combination was favored in the Curtin–Hammett pre-equilibrium in the resolution of the benzyl-substituted aminopentene **3b** with catalyst **2b** (Table 3, entry 9). The high efficiency in the kinetic resolution of **3b** with **2c** was achieved through a combination of high relative rate, k_{fast}/k_{slow}, and a Curtin–Hammett pre-equilibrium in favor of the matching substrate–catalyst pair ($K^{dias} > 1$) (Table 3, entry 10). Although the pre-equilibrium was slightly in favor of the matching substrate–catalyst pair for catalyst **2e**, the low k_{fast}/k_{slow} ratio resulted in an overall low efficiency of the kinetic resolution of substrate **3b** (Table 3, entry 11). While the diastereoselectivities remained high for the matching pair of substrate (*S*)-**3b** and the (*S*)-catalyst, significantly lower *trans*/*cis* diastereoselectivities were observed for the mismatching pair with all tested catalysts (Table 3, entries 9–11), in contrast to previous observations for catalyst (*S*)-**1a-Y**.[15]

High diastereoselectivities of up to 50:1 were observed for the phenyl-substituted aminopentene **3c** with all binaphtholate catalysts (Table 3, entries 12–16). Although the cyclization rate of the matching substrate–catalyst pair, involving substrate (*S*)-**3c** and catalyst (*S*)-**1a-Y**, was about three times faster than that of (*S*)-**3c** and (*S*)-**2c** at 60 °C, a higher k_{fast}/k_{slow} ratio was observed for **3c** with **2c** [k_{fast}/k_{slow} = 15.7(7) vs. 7.1 with **1a-Y**] (Table 3, entries 12 and 14). As a result, the cyclohexyldiphenylsilyl-substituted binaphtholate catalyst **2c** was more efficient in the kinetic resolution of **3c** in comparison to **1a-Y**.

The alkylarylsilyl-substituted binaphtholate catalysts **2b**, **2c**, and **2e** behaved quite differently in the kinetic resolution of the cyclohexyl-substituted aminopentene **3d** compared to the triphenylsilyl-substituted binaphtholate catalyst **1a-Y**. The k_{fast}/k_{slow} ratios were significantly lower for **2b**, **2c**, and **2e** com-

pared to **1a-Y**; however, this deficiency is overcompensated by a Curtin–Hammett pre-equilibrium in favor of the matching substrate–catalyst pair for **2b**, **2c**, and **2e** ($K^{dias} > 1$), whereas in case of **1a-Y**[15] the pre-equilibrium favors the mismatching substrate–catalyst pair (compare Table 3 entries 18–20 with entry 17). As a result, **2b**, **2c**, and **2e** are slightly more efficient catalysts for the kinetic resolution of **3d** in comparison to **1a-Y**.

The Eyring plot for k_{fast} and k_{slow} (Figure 8) provided an access to the activation parameters for the hydroamination/cyclization of (*S*)-**3a** using (*R*)-**2c** (matching substrate–catalyst pair) [$\Delta H^{\ddagger}$ = 43(6) kJ mol^{-1}, $\Delta S^{\ddagger}$ = –137(18) J mol^{-1} K^{-1}]. Because the reaction of (*S*)-**3a** and (*S*)-**2c** (mismatching substrate–catalyst pair) afforded the products with low *trans*/*cis* diastereoselectivities, the activation parameters for each diastereomer were obtained [*trans*: $\Delta H^{\ddagger}$ = 52(3) kJ mol^{-1}, $\Delta S^{\ddagger}$ = –138(8) J mol^{-1} K^{-1}; *cis*: $\Delta H^{\ddagger}$ = 52(5) kJ mol^{-1}, $\Delta S^{\ddagger}$ = –135(16) J mol^{-1} K^{-1}]. The activation parameters for the matching and mismatching substrate-catalyst pair seem to be in a similar range to those obtained previously for **3a** with catalyst **1a-Y** [matching pair: $\Delta H^{\ddagger}$ = 47.3(3.5) kJ mol^{-1}, $\Delta S^{\ddagger}$ = –128(11) J mol^{-1} K^{-1}; mismatching pair: $\Delta H^{\ddagger}$ = 54.9(3.1) kJ mol^{-1}, $\Delta S^{\ddagger}$ = –121(9) J mol^{-1} K^{-1}].[15] The negative activation entropy is indicative of a highly organized transition state.[12d,15,21]

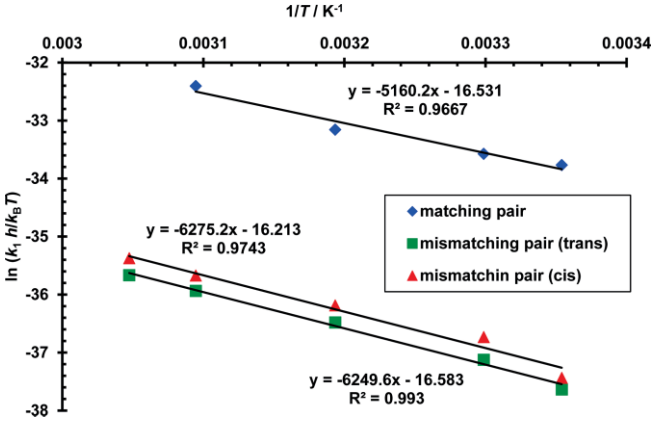

Figure 8. Eyring plot for the hydroamination/cyclization of (*S*)-**3a** using (*R*)-**2c** (matching pair) and (*S*)-**2c** (mismatching pair).

Stereomodel for the Kinetic Resolution of α-Substituted Aminopentenes

According to the proposed stereomodel for the kinetic resolution of α-substituted aminopentenes using binaphtholate rare-earth metal catalysts, the diastereomers can be obtained via possible cyclization pathways as depicted in Scheme 3.[12d,15]

The stereomodel for the kinetic resolution is in agreement with the general stereomodel for enantioselective intramolecular hydroamination of aminopentenes by (*R*)-binaphtholate rare-earth metal catalysts, in which the Ln–N bond preferentially approaches the *re* face of the olefin.[12d] In case of the matching substrate–catalyst pair, the α-substituent of the aminoalkene rests in an equatorial position of the seven-membered chair-like transition state in the conformation that facilitates the approach of the Ln–N bond to the olefin from the *re* face (Scheme 3, pathway **C**). In case of the mismatching substrate-catalyst combination, the sterically unfavorable interaction between the substrate and the alkylarylsilyl-substituent of the binaphtholate ligand restricts the approach of the Ln–N bond to the olefin from the *si* face (Scheme 3, pathway **A**). Pathway **B** provides an alternative to pathway **A**, allowing the mismatching substrate-catalyst complex to avoid the steric interaction between the substrate and the bulky silyl group. However, pathway **B** requires the α-substituent of the aminopentene to rest in an axial position, which leads to an unfavorable 1,3-diaxial interaction in the chair-like transition state and possibly steric interaction between the α-substituent R of the substrate and an alkylarylsilyl-substituent of the binaphtholate ligand, if the α-substituent R is sufficiently large.

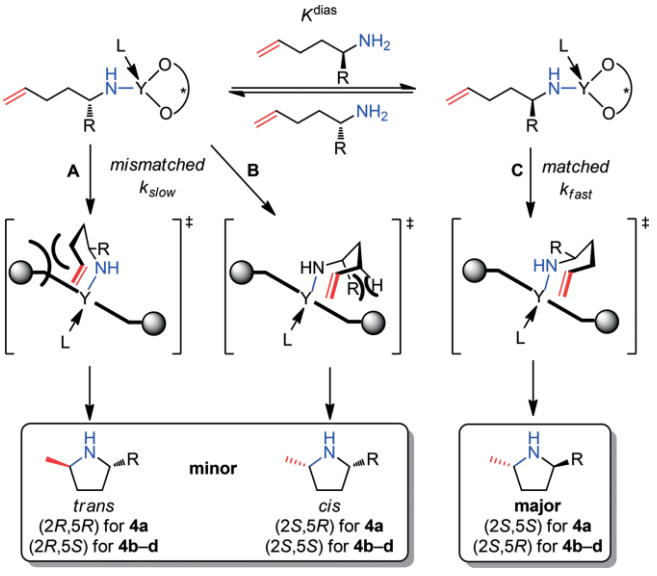

Scheme 3. Proposed stereomodel for the kinetic resolution of α-substituted aminopentenes with (*R*)-binaphtholate yttrium catalysts.[12d,15] L = aminoalkene substrate or hydroamination product.

Pathway **B** accounts for the significantly reduced diastereoselectivities which were observed for the mismatching substrate-catalyst combinations when using catalysts **2b**, **2c**, and **2e**. Moreover, the cyclization of the mismatching substrate–catalyst pairs (*S*)-**3a** with (*S*)-**2c**, (*S*)-**3d** with (*S*)-**2b**, and (*S*)-**3d** with (*S*)-**2c** generated predominantly the *cis*-pyrrolidine products; thus, pathway **B** becomes the preferred pathway. The exceptionally high efficiency in the kinetic resolution of the methyl-substituted aminopentene **3a** with **2c** results from the Curtin–Hammett pre-equilibrium in favor of the matching substrate-catalyst complex and a high k_{fast}/k_{slow} ratio.

The large *trans*/*cis* diastereoselectivities, exceeding 50:1, observed for the phenyl-substituted aminopentene **3c** in comparison to the alkyl-substituted aminopentenes **3a**, **3b**, and **3d**, may result from a coordinative interaction of the phenyl-substituent of **3c** with the metal center[22] or a π-interaction of the phenyl-substituent with a naphthyl ring of the binaphtholate ligand.

Conclusions

The kinetic resolution of α-substituted aminopentenes via asymmetric hydroamination/cyclization was studied using rare-

earth metal catalysts based on 3,3′-bis(alkylarylsilyl)-substituted binaphtholate ligands. In general the cyclohexyldiphenylsilyl-substituted binaphtholate catalyst (*R*)-**2c** displays high efficiency in the kinetic resolution of the methyl-, benzyl-, and phenyl-substituted substrates **3a**, **3b**, and **3c**, respectively. The highest resolution factor of up to 90(5) was observed for **3a** using (*R*)-**2c**. Despite having a favorable Curtin–Hammett pre-equilbrium, the cyclohexyl-substituted aminopentene **3d** exhibits low efficiency in the kinetic resolution with all binaphtholate catalysts screened in this study as a result of a low k_{fast}/k_{slow} ratio.

The activation parameters for the cyclization of (*S*)-**3a** with complex (*R*)-**2c** (matching substrate–catalyst pair) and (*S*)-**3a** with complex (*S*)-**2c** (mismatching substrate–catalyst pair) are in line with the previously reported data obtained for the cyclization of **3a** using complex **1a-Y**.[15] It is noteworthy that the mismatching substrate-catalyst combination of (*S*)-**3a** and (*S*)-**2c** preferentially affords the *cis*-product. The kinetic resolution parameters show that high efficiency in the kinetic resolution of the methyl-substituted **3a** with **2c** stems from the Curtin–Hammett pre-equilibrium in favor of the matching substrate-catalyst combination and a high k_{fast}/k_{slow} ratio.

Experimental Section

General Considerations: All operations were performed under an inert atmosphere of nitrogen or argon using standard Schlenk-line or glovebox techniques. Solvents and reagents were purified as stated previously.[12d] Complexes **2a**–**2e**,[12f] substrates hex-5-en-2-amine (**3a**),[23] 1-phenylhex-5-en-2-amine (**3b**),[12d] 1-phenylpent-4-en-1-amine (**3c**),[12d] and 1-cyclohexylpent-4-en-1-amine (**3d**),[15] were prepared according to previously described procedures. The substrates were distilled twice from finely powder CaH_2, stored over molecular sieves, and kept in the fridge of a glovebox. (*S*)-(+)-α-Methoxy-α-trifluoro-methylphenylacetic acid (Mosher acid) was transformed to the corresponding (*R*)-Mosher acid chloride using oxalyl chloride/DMF in hexanes.[24] Enantiomeric excess for **3a**–**3d** was measured by ^{19}F NMR spectroscopy of the corresponding Mosher amides as reported previously.[12d,15]

General Procedure for NMR-Scale Kinetic Resolution of Chiral α-Substituted Aminopentenes: In a glove box, a screw cap NMR tube was charged with racemic aminoalkene (20.0 mg, 0.10–0.20 mmol), ferrocene (3.0 mg, 16.1 μmol), [D_6]benzene (to give a total volume of 0.5 mL), and catalysts (2.0 mol-% with respect to racemic aminoalkene, 2.0–4.0 μmol, 0.060 M in [D_6]benzene). The NMR tube was capped, immediately removed from the glovebox, and shaken well to dissolve ferrocene. The reaction mixture was heated in a thermostatic oil bath, if required. The conversion was monitored by ^1H NMR spectroscopy by following the disappearance of the olefinic signals of the substrate relative to the internal standard ferrocene. The reaction was stopped after ca. 50 % conversion was achieved. The aminoalkene starting material was isolated in form of the hydrochloride salt and enantiomeric excess was determined using the previously reported procedure.[12c,12d]

General Procedure for Preparation of Chiral α-Substituted Aminopentenes by Kinetic Resolution: In a glovebox, a 20 mL vial was charged with the racemic aminoalkenes (**3c**: 0.80 g, 5.0 mmol; **3a**, **3b**, and **3d**: 1.50 g, 8.0–9.0 mmol), benzene (5.0 mL), and **2c** (0.5–0.9 mL of solution, 0.20 M in benzene, 0.10–0.18 mmol, 2.0 mol-%). The vial was kept at 25 °C (**3a**, **3b**, and **3d**) or heated to 40 °C (**3c**). Small aliquots (20 μL) were syringed to NMR tubes, which was then diluted with $CDCl_3$ (0.55 mL), and a ^1H NMR spectrum was recorded to monitor the conversion. The reaction was stopped after enantiomeric excess of the starting material reached at least 95 %*ee*, determined by ^{19}F NMR spectroscopy of its corresponding Mosher amide at 40–65 °C. The chiral α-substituted aminopentenes were isolated by the standard benzaldimine work-up procedure[12c,12d] and were purified by vacuum distillation from CaH_2.

(2*S*)-Hex-5-en-2-amine [(*S*)-3a]: This compound was prepared by kinetic resolution using (*S*)-**2c** at 25 °C, 52 % conversion after 9 h. The enantioenriched starting material was recovered as colorless oil (38 % yield, bp 114–116 °C at 760 Torr, 95 % *ee*). The NMR spectra are in agreement with those of *rac*-hex-5-en-2-amine.[23]

(2*S*)-1-Phenylhex-5-en-2-amine [(*S*)-3b]: This compound was prepared by kinetic resolution using (*R*)-**2c** at 25 °C, 57 % conversion after 22.5 h. The enantioenriched starting material was recovered as colorless oil (40 % yield, 95 % *ee*, bp 103 °C at 0.2 Torr). The NMR spectra are in agreement with those of *rac*-1-phenylhex-5-en-2-amine.[12d]

(1*S*)-1-Phenylpent-4-en-1-amine (3c): This compound was prepared by kinetic resolution using (*R*)-**2c** at 40 °C, 54 % conversion after 31 h. The enantioenriched starting material was recovered as colorless oil (40 % yield, 97 % *ee*). The NMR spectra are in agreement with those of *rac*-1-phenylpent-4-enylamine.[12d]

(1*S*)-1-Cyclohexylpent-4-en-1-amine [(*S*)-3d]: This compound was prepared by kinetic resolution using (*R*)-**2c** at 25 °C, 77 % conversion after 9.5 hours. The enantioenriched starting material was recovered as colorless oil (18 % yield, 95 % *ee*, bp 80 °C at 0.2 Torr). The NMR spectra are in agreement with those of *rac*-1-cyclohexylpent-4-en-1-amine.[15]

General Procedure for Kinetic Catalytic Hydroamination/cyclization Reactions: In a glovebox, a screw cap NMR tube were charged with a solution of the enantioenriched α-substituted aminopentene (2.0 w% in [D_6]benzene, 200–375 μL, 58.0–74.0 μmol), ferrocene (3.0 mg), [D_6]benzene (to give a total volume of 500 μL), and catalyst (2.0 mol-%, 1.16–1.48 μmol, 21–24 μL stock solution in [D_6]-benzene). The tube was placed in either 400 or 500 MHz NMR thermostatic probe with temperature of 25–55 °C and an arrayed experiment was set up to record ^1H NMR spectra automatically in time intervals (30 sec, 1 min, 3 min, 5 min, or 10 min). The conversion was determined based on the disappearance of the olefinic signals of the substrate relative to the internal standard ferrocene. The linear part of the data was fit by least square analysis and k_{obs} was determined from the slope α of a plot of concentration of amine (M) vs. time (min).

Acknowledgments

This work was supported by the National Science Foundation through an NSF CAREER Award (CHE 0956021).

Keywords: Asymmetric catalysis · Hydroamination · Kinetic resolution · Reaction mechanisms · Rare earths

[1] a) A. Ricci, *Modern Amination Methods*, Wiley-VCH, **2000**; b) A. Ricci, *Amino Group Chemistry: From Synthesis to the Life Sciences*, Wiley-VCH, **2008**; c) *Chiral Amine Synthesis: Methods, Developments and Applications*; (Ed.: T. Nugent), Wiley-VCH: Weinheim, Germany, **2010**.

[2] For general reviews on hydroamination see: a) T. E. Müller, M. Beller, *Chem. Rev.* **1998**, *98*, 675–704; b) J. J. Brunet, D. Neibecker in *Catalytic Heterofunctionalization from Hydroamination to Hydrozirconation* (Eds.: A. Togni, H. Grützmacher), Wiley-VCH, Weinheim, **2001**, pp. 91–141; c) T. E. Müller, K. C. Hultzsch, M. Yus, F. Foubelo, M. Tada, *Chem. Rev.* **2008**, *108*, 3795–3892; d) S. Doye in *Science of Synthesis*, *Vol. 40a* (Ed.: D. Enders), Thieme, Stuttgart, **2009**, pp. 241–304; e) A. L. Reznichenko, K. C. Hultzsch, *Top. Organomet. Chem.* **2013**, *43*, 51–114; f) N. Nishina, Y. Yamamoto, *Top. Organomet. Chem.* **2013**, *43*, 115–143; g) A. L. Reznichenko, K. C. Hultzsch in *Organic Reactions*, *Vol. 88* (Eds.: S. E. Denmark, A. Charette), Wiley: Hoboken, NJ, **2016**, pp. 1–554.

[3] Reviews on rare-earth-metal-catalyzed hydroaminations: a) S. Hong, T. J. Marks, *Acc. Chem. Res.* **2004**, *37*, 673–686; b) A. L. Reznichenko, K. C. Hultzsch, *Struct. Bonding (Berlin)* **2010**, *137*, 1–48; c) A. A. Trifonov, I. V. Basalov, A. A. Kissel, *Dalton Trans.* **2016**, *45*, 19172–19193.

[4] Reviews on Group 4- and actinide-catalyzed hydroaminations: a) I. Bytschkov, S. Doye, *Eur. J. Org. Chem.* **2003**, 935–946; b) F. Pohlki, S. Doye, *Chem. Soc. Rev.* **2003**, *32*, 104–114; c) S. Doye, *Synlett* **2004**, 1653–1672; d) A. L. Odom, *Dalton Trans.* **2005**, 225–233; e) R. Severin, S. Doye, *Chem. Soc. Rev.* **2007**, *36*, 1407–1420; f) A. V. Lee, L. L. Schafer, *Eur. J. Inorg. Chem.* **2007**, 2243–2255; g) P. Eisenberger, L. L. Schafer, *Pure Appl. Chem.* **2010**, *82*, 1503–1515; h) T. Andreas, M. S. Eisen, *Chem. Soc. Rev.* **2008**, *37*, 550–567.

[5] Reviews on alkali- and alkaline-earth-metal-catalyzed hydroaminations: a) J. Seayad, A. Tillack, C. G. Hartung, M. Beller, *Adv. Synth. Catal.* **2002**, *344*, 795–813; b) S. Harder, *Chem. Rev.* **2010**, *110*, 3852–3876; c) A. G. M. Barrett, M. R. Crimmin, M. S. Hill, P. A. Procopiou, *Proc. R. Soc. London Ser. A* **2010**, *466*, 927–963; d) M. R. Crimmin, M. S. Hill, *Top. Organomet. Chem.* **2013**, *45*, 191–241.

[6] Reviews on late transition metal-based catalysts: a) M. Beller, C. Breindl, M. Eichberger, C. G. Hartung, J. Seayad, O. R. Thiel, A. Tillack, H. Trauthwein, *Synlett* **2002**, 1579–1594; b) J. F. Hartwig, *Pure Appl. Chem.* **2004**, *76*, 507–516; c) R. A. Widenhoefer, X. Han, *Eur. J. Org. Chem.* **2006**, 4555–4563; d) J. J. Brunet, N. C. Chu, M. Rodriguez-Zubiri, *Eur. J. Inorg. Chem.* **2007**, 4711–4722; e) K. D. Hesp, M. Stradiotto, *ChemCatChem* **2010**, *2*, 1192–1207; f) J. Jenter, A. Lühl, P. W. Roesky, S. Blechert, *J. Organomet. Chem.* **2010**, *695*, 406–418; g) V. Rodriguez-Ruiz, R. Carlino, S. Bezzenine-Lafollee, R. Gil, D. Prim, E. Schulz, J. Hannedouche, *Dalton Trans.* **2015**, *44*, 12029–12059; h) L. Huang, M. Arndt, K. Gooßen, H. Heydt, L. J. Gooßen, *Chem. Rev.* **2015**, *115*, 2596–2697; i) For a recent example of an iron-catalyzed hydroamination of aminoalkenes, see: C. Lepori, E. Bernoud, R. Guillot, S. Tobisch, J. Hannedouche, *Chem. Eur. J.* **2019**, *25*, 835–844.

[7] For reviews on photocatalytic hydroaminations see: a) K. A. Margrey, D. A. Nicewicz, *Acc. Chem. Res.* **2016**, *49*, 1997–2006; b) D. Menigaux, P. Belmont, E. Brachet, *Eur. J. Org. Chem.* **2017**, 2008–2055.

[8] a) For a review on the asymmetric formal hydroamination of alkenes using copper hydride catalysts see: M. T. Pirnot, Y. M. Wang, S. L. Buchwald, *Angew. Chem. Int. Ed.* **2016**, *55*, 48–57; *Angew. Chem.* **2016**, *128*, 48–57; b) For a review on the Cope-type hydroamination see: A. M. Beauchemin, *Org. Biomol. Chem.* **2013**, *11*, 7039–7050.

[9] For reviews on asymmetric hydroamination see: a) P. W. Roesky, T. E. Müller, *Angew. Chem. Int. Ed.* **2003**, *42*, 2708–2710; *Angew. Chem.* **2003**, *115*, 2812–2814; b) K. C. Hultzsch, *Adv. Synth. Catal.* **2005**, *347*, 367–391; c) I. Aillaud, J. Collin, J. Hannedouche, E. Schulz, *Dalton Trans.* **2007**, 5105–5118; d) G. Zi, *Dalton Trans.* **2009**, 9101–9109; e) S. R. Chemler, *Org. Biomol. Chem.* **2009**, *7*, 3009–3019; f) G. Zi, *J. Organomet. Chem.* **2011**, *696*, 68–75; g) J. Hannedouche, J. Collin, A. Trifonov, E. Schulz, *J. Organomet. Chem.* **2011**, *696*, 255–262; h) J. Hannedouche, E. Schulz, *Chem. Eur. J.* **2013**, *19*, 4972–4985; i) A. L. Reznichenko, A. J. Nawara-Hultzsch, K. C. Hultzsch, *Top. Curr. Chem.* **2013**, *343*, 191–260; j) C. Michon, M. A. Abadie, F. Medina, F. Agbossou-Niedercorn, *J. Organomet. Chem.* **2017**, *847*, 13–27.

[10] For selected examples of highly enantioselective intramolecular hydroamination of aminoalkenes see: a) M. C. Wood, D. C. Leitch, C. S. Yeung, J. A. Kozak, L. L. Schafer, *Angew. Chem. Int. Ed.* **2007**, *46*, 354–358; *Angew. Chem.* **2007**, *119*, 358–362; b) X. Shen, S. L. Buchwald, *Angew. Chem. Int. Ed.* **2010**, *49*, 564–567; *Angew. Chem.* **2010**, *122*, 574–577; c) K. Manna, M. L. Kruse, A. D. Sadow, *ACS Catal.* **2011**, *1*, 1637–1642; d) Y. Zhang, W. Yao, H. Li, Y. Mu, *Organometallics* **2012**, *31*, 4670–4679; e) X. Zhang, T. J. Emge, K. C. Hultzsch, *Angew. Chem. Int. Ed.* **2012**, *51*, 394–398; *Angew. Chem.* **2012**, *124*, 406–410; f) K. Manna, W. C. Everett, G. Schoendorff, A. Ellern, T. L. Windus, A. D. Sadow, *J. Am. Chem. Soc.* **2013**, *135*, 7235–7250; g) Z. Chai, D. Hua, K. Li, J. Chu, G. Yang, *Chem. Commun.* **2014**, *50*, 177–179; h) L. Hussein, N. Purkait, M. Biyikal, E. Tausch, P. W. Roesky, *Chem. Commun.* **2014**, *50*, 3862–3864; i) X. Zhou, B. Wei, X. L. Sun, Y. Tang, Z. Xie, *Chem. Commun.* **2015**, *51*, 5751–5753; j) For the highly enantioselective intermolecular hydroamination of cyclopropenes see: H. L. Teng, Y. Luo, B. Wang, L. Zhang, M. Nishiura, Z. Hou, *Angew. Chem. Int. Ed.* **2016**, *55*, 15406–15410; *Angew. Chem.* **2016**, *128*, 15632–15636.

[11] For selected examples of highly enantioselective intramolecular hydroamination reactions of aminodienes and aminoallenes see: a) R. L. LaLonde, B. D. Sherry, E. J. Kang, F. D. Toste, *J. Am. Chem. Soc.* **2007**, *129*, 2452–2453; b) G. L. Hamilton, E. J. Kang, M. Mba, F. D. Toste, *Science* **2007**, *317*, 496–499; c) Z. Zhang, C. F. Bender, R. A. Widenhoefer, *Org. Lett.* **2007**, *9*, 2887–2889; d) R. L. LaLonde, Z. J. Wang, M. Mba, A. D. Lackner, F. D. Toste, *Angew. Chem. Int. Ed.* **2010**, *49*, 598–601; *Angew. Chem.* **2010**, *122*, 608–611; e) N. D. Shapiro, V. Rauniyar, G. L. Hamilton, J. Wu, F. D. Toste, *Nature* **2011**, *470*, 245–249; f) O. Kanno, W. Kuriyama, Z. J. Wang, F. D. Toste, *Angew. Chem. Int. Ed.* **2011**, *50*, 9919–9922; *Angew. Chem.* **2011**, *123*, 10093–10096.

[12] a) D. V. Gribkov, K. C. Hultzsch, F. Hampel, *Chem. Eur. J.* **2003**, *9*, 4796–4810; b) D. V. Gribkov, F. Hampel, K. C. Hultzsch, *Eur. J. Inorg. Chem.* **2004**, 4091–4101; c) D. V. Gribkov, K. C. Hultzsch, *Chem. Commun.* **2004**, 730–731; d) D. V. Gribkov, K. C. Hultzsch, F. Hampel, *J. Am. Chem. Soc.* **2006**, *128*, 3748–3759; e) A. L. Reznichenko, K. C. Hultzsch, *Organometallics* **2013**, *32*, 1394–1408; f) H. N. Nguyen, H. Lee, S. Audörsch, A. L. Reznichenko, A. J. Nawara-Hultzsch, B. Schmidt, K. C. Hultzsch, *Organometallics* **2018**, *37*, 4358–4379. See also: g) X. Yu, T. J. Marks, *Organometallics* **2007**, *26*, 365–376.

[13] A. L. Reznichenko, H. N. Nguyen, K. C. Hultzsch, *Angew. Chem. Int. Ed.* **2010**, *49*, 8984–8987; *Angew. Chem.* **2010**, *122*, 9168–9171.

[14] For reviews on kinetic resolution see: a) H. B. Kagan, J. C. Fiaud, *Top. Stereochem.* **1988**, *18*, 249–330; b) E. Vedejs, M. Jure, *Angew. Chem. Int. Ed.* **2005**, *44*, 3974–4001; *Angew. Chem.* **2005**, *117*, 4040–4069; c) H. Pellissier, *Adv. Synth. Catal.* **2011**, *353*, 1633–1666.

[15] A. L. Reznichenko, F. Hampel, K. C. Hultzsch, *Chem. Eur. J.* **2009**, *15*, 12819–12827. For the application of NOBIN-based aminophenolate complexes in the kinetic resolution of aminoalkenes see ref.[12e]

[16] a) For the gold-catalyzed dynamic kinetic resolution of aminoallenes via hydroamination/cyclization see: Z. Zhang, C. F. Bender, R. A. Widenhoefer, *J. Am. Chem. Soc.* **2007**, *129*, 14148–14149; b) For the stereoconvergent, intermolecular asymmetric hydroamination of racemic allenes see: K. L. Butler, M. Tragni, R. A. Widenhoefer, *Angew. Chem. Int. Ed.* **2012**, *51*, 5175–5178; *Angew. Chem.* **2012**, *124*, 5265–5268; c) For the desymmetrization of aminodialkenes and aminodialkynes see: K. Manna, N. Eedugurala, A. D. Sadow, *J. Am. Chem. Soc.* **2015**, *137*, 425–435; d) For the diastereodivergent asymmetric carboamination/annulation of cyclopropenes with aminoalkenes see: H. L. Teng, Y. Luo, M. Nishiura, Z. Hou, *J. Am. Chem. Soc.* **2017**, *139*, 16506–16509.

[17] For rare-earth-metal-catalyzed kinetic resolution processes other than hydroamination, see for example: a) M.-H. Lin, T. V. RajanBabu, *Org. Lett.* **2002**, *4*, 1607–1610; b) C. I. Maxwell, K. Shah, P. V. Samuleev, A. A. Neverov, R. S. Brown, *Org. Biomol. Chem.* **2008**, *6*, 2796–2803; c) L. Zhou, X. Liu, J. Ji, Y. Zhang, X. Hu, L. Lin, X. Feng, *J. Am. Chem. Soc.* **2012**, *134*, 17023–17026; d) L. Zhou, X. Liu, J. Ji, Y. Zhang, W. Wu, Y. Liu, L. Lin, X. Feng, *Org. Lett.* **2014**, *16*, 3938–3941; e) Y. Zhang, X. Liu, L. Zhou, W. Wu, T. Huang, Y. Liao, L. Lin, X. Feng, *Chem. Eur. J.* **2014**, *20*, 15884–15890; f) B. Wu, J. C. Gallucci, J. R. Parquette, T. V. RajanBabu, *Chem. Sci.* **2014**, *5*, 1102–1117; g) Y. Xu, K. Kaneko, M. Kanai, M. Shibasaki, S. Matsunaga, *J. Am. Chem. Soc.* **2014**, *136*, 9190–9194; h) T. Huang, L. Lin, X. Hu, J. Zheng, X. Liu, X. Feng, *Chem. Commun.* **2015**, *51*, 11374–11377; i) N. Li, B. T. Guan, *Adv. Synth. Catal.* **2017**, *359*, 3526–3531; j) H. K. Kisan, R. B. Sunoj, *ACS Catal.* **2018**, *8*, 7633–7644.

[18] Resolution factors > 50 are difficult to determine with sufficient precision based on a single data point. A better estimate for these large *f* values can be obtained from linear regression of several data points (vide infra).

[19] For the detailed derivation of the underlying equations see ref. [12d].

[20] For simplification we assume that k_R/k_S represents k_{fast}/k_{slow} for all substrates. Note however, that for substrate **3a** the *S* enantiomer is the faster reacting enantiomer when using the (*R*)-binaphtholate catalysts.
[21] M. R. Gagné, C. L. Stern, T. J. Marks, *J. Am. Chem. Soc.* **1992**, *114*, 275–294.
[22] M. N. Bochkarev, *Chem. Rev.* **2002**, *102*, 2089–2117.
[23] J. Y. Kim, T. Livinghouse, *Org. Lett.* **2005**, *7*, 4391–4393.
[24] P. M. Smith, E. J. Thomas, *J. Chem. Soc., Perkin Trans. 1* **1998**, 3541–3556.

Received: January 22, 2019